

Bipyridyl oxadiazoles as efficient and durable electron-transporting and hole-blocking molecular materials

Musubu Ichikawa,^{*a} Taro Kawaguchi,^a Kana Kobayashi,^a Tetsuzo Miki,^b Kenji Furukawa,^a Toshiki Koyama^a and Yoshio Taniguchi^a

Received 27th July 2005, Accepted 18th October 2005

First published as an Advance Article on the web 4th November 2005

DOI: 10.1039/b510720b

We have demonstrated new and efficient electron transporting (ET) and hole blocking (HB) materials for organic light-emitting devices (OLEDs). The bipyridyl-substituted oxadiazole derivatives can form a stable glassy state with glass transition temperatures greater than 100 °C. The bipyridyl-substituted oxadiazole derivatives have excellent ET, HB and electron accepting ability and also exhibit electrical operation durability. Bipyridyl-substituted oxadiazoles are a promising candidate for ET and HB materials for OLEDs.

Introduction

Organic light-emitting devices (OLEDs) have received much attention due to their potential applications to flat panel displays. OLEDs are generally composed of functionally divided organic multi-layers, *e.g.*, hole transporting (HT), emissive, and electron transporting (ET) layers, and so on.^{1,2} In the last decade, many kinds of amorphous molecular semiconductor materials,^{3,4} working as HT materials^{5–8} and ET materials,^{9–14} have been proposed, and HT molecular semiconducting materials have become practical due to their high charge carrier mobility and excellent operational durability. On the other hand, there have been few reports of ET organic semiconducting amorphous materials with high performance (high-speed transportation of electrons, easy injection of electrons from the cathode, and good operational durability).¹² Tris(8-hydroxyquinolino)aluminum(III) (Alq), which is the historical material reported in the first bright OLEDs by Tang *et al.* in 1987, is still conventionally used as an ET material regardless of its slow electron mobility¹⁵ because it exhibits high operational durability. However, as a reflection of the imbalanced performance between ET and HT materials, electron-feeding from the cathode into an emissive layer control device characterizes OLEDs. Therefore, the development of efficient ET organic materials is a challenge of high priority.

Efficient ET materials provide some advantages, such as lowering the operating voltage and power consumption. Moreover, if the ET materials have wide band gaps, in other words, deeper highest occupied molecular orbitals (HOMO), such ET materials can also work as hole blocking (HB) materials. The complete confinement of a hole in an emissive layer by the HB layer raises the quantum efficiencies of electroluminescence (EL). Oxadiazole is a well-known electron accepting component for building ET materials with high electron mobility, and oxadiazole derivatives (OXDs) exhibit

wide band gap properties because oxadiazole restricts extensions of π -conjugation beyond the ring even if the molecule is co-planar.^{4,16} Accordingly, OXDs are a promising ET and HB material for OLEDs, but it has been widely accepted that OXDs should acquire durability capacity for long-term operations in OLEDs.¹⁰ Here, we show that bipyridyl-substituted oxadiazole compounds have efficient electron-transporting and hole-blocking properties with high thermal stability and practical operation durability.

Experimental

Measurements

¹H NMR spectra were recorded on a JEOL JNM-EX270 spectrometer (270 MHz). Elemental analysis was carried out with a Yanaco MT-3 CHNcoder. Thermal analysis was performed on a Seiko Instruments DSC-6200 at a heating rate of 10 °C min⁻¹ for differential scanning calorimetry (DSC) under nitrogen. X-Ray diffraction (XRD) patterns of thin films were measured using Cu K α radiation with 40 kV and 150 mA. Ultraviolet (UV) and visible absorption spectra and fluorescence spectra were recorded with a Shimadzu UV-3150 spectrophotometer and a JASCO FP-750 spectrofluorometer, respectively. The HOMO level was measured with a Riken Keiki AC-3 photoelectron emission spectrometer, where the HOMO level was defined as being equal to the ionization potential measured by photoelectron emission spectroscopy. The lowest unoccupied molecular orbital (LUMO) level was estimated from the HOMO level and the band gap, which was determined by the absorption edge of the UV and the visible absorption spectrum of the neat thin film. Neat thin films prepared by vacuum deposition on quartz glasses at a pressure of 6 \times 10⁻⁴ Pa or less were used as samples for XRD, UV-visible absorption, fluorescence, and photoelectron emission spectroscopy.

Materials

We synthesized new bipyridyl-substituted oxadiazole compounds, 1,3-bis[(2-(2,2'-bipyridin-6-yl)-1,3,4-oxadiazol-5-yl)]benzene

^aDepartment of Functional Polymer Science, Faculty of Textile Science and Technology, Shinshu University, 3-15-1 Tokita, Ueda, Nagano 386-8567, Japan. E-mail: musubu@gipc.shinshu-u.ac.jp

^bHodogaya Chemical Co., Ltd., Miyukigaoka 45, Tsukuba, Ibaraki 305-0841, Japan

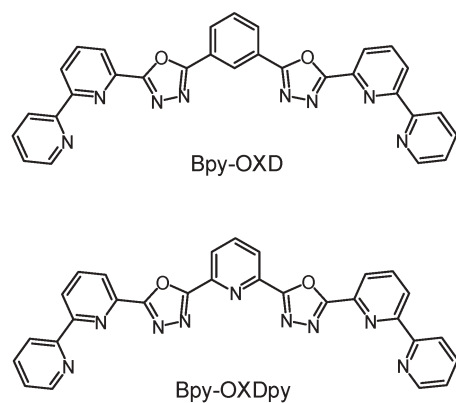


Fig. 1 Chemical structures of new bipyridyl substituted oxadiazole compounds and other materials used in this study.

(Bpy-OXD) and 2,6-bis[2-(2,2'-bipyridin-6-yl)-1,3,4-oxadiazol-5-yl]pyridine (Bpy-OXDpy), whose chemical structures are shown in Fig. 1, from the tetrazole intermediate *via* intramolecular ring formation¹⁷ as described below. They were purified by silica gel column chromatography to give white crystals, whose structures were confirmed by NMR spectroscopy and elemental analysis. Further purification was carried out with temperature gradient sublimation in a flow stream of 99.999% argon gas before use. Other chemicals used in this study, whose structures are shown in Fig. 2a, were from Nippon Steel Chemical (Alq, NPB and CuPc) and H.W. Sands (OXD-7). These materials were used with no further purification because they were sublimation grade.

1,3-Bis[2-(2,2'-bipyridin-6-yl)-1,3,4-oxadiazol-5-yl]benzene (Bpy-OXD). 6-(2*H*-Tetrazol-5-yl)-2,2'-bipyridine, 0.63 g in 10 ml dry pyridine, was stirred. Then, 0.29 g of isophthaloyl dichloride was added slowly and refluxed at 115 °C for 6 hours. After cooling, the reaction mixture was poured into 100 ml of water. The white precipitate was isolated by filtration, washed with water, and vacuum dried at 80 °C. Silica gel column chromatography (CHCl₃–MeOH = 20 : 1) gave 0.62 g of pure white powder with an 81% yield. δ_{H} (270 MHz; CDCl₃; Me₄Si) 9.08 (1 H, s), 8.72 (2 H, br d, *J* 4.9), 8.65 (4 H, br d, *J* 8.1) 8.47 (2 H, br d, *J* 7.8), 8.35 (6 H, d, *J* 7.8), 8.05 (2 H, t, *J* 7.8), 7.86–7.77 (3 H, m), 7.35 (2 H, dd, *J* 4.9). Elemental analysis: calc. for C₃₀H₁₈N₈O₂: C = 68.96, H = 3.47, N = 21.44. Found: C = 69.27, H = 3.63, N = 21.30%. ν_{max} (KBr)/cm⁻¹ 1585, 1541, 1456 and 1427. *m/z* (EI, low resolution) 522 (M⁺ requires 522.16), 444 (M⁺ – pyridyl. C₂₅H₁₄N₇O₂ requires 444.12) and others.

2,6-Bis[2-(2,2'-bipyridin-6-yl)-1,3,4-oxadiazol-5-yl]pyridine (Bpy-OXDpy). 6-(2*H*-Tetrazol-5-yl)-2,2'-bipyridine, 0.50 g in 10 ml dry pyridine, was stirred. Then, 0.26 g of 2,6-pyridine-carbonyl-dichloride was added slowly and refluxed at 110 °C for 9 hours. After cooling, the reaction mixture was poured into 100 ml of water. The white precipitate was isolated by filtration, washed with water, and vacuum dried at 80 °C. Silica gel column chromatography (CHCl₃–MeOH = 20 : 1) gave 0.12 g of pure white powder with a 24% yield. δ_{H} (270 MHz; CDCl₃; Me₄Si) 8.01–8.65 (13 H, m), 7.67 (2 H,

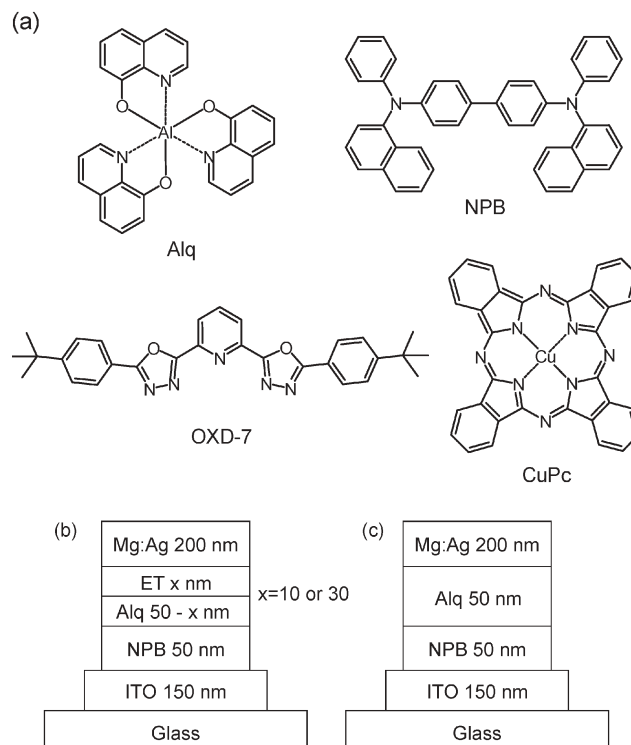


Fig. 2 (a) Chemical structures of OLED materials used in this study and device structures of fabricated OLEDs with Bpy-OXD as ET layers (b) and the reference device (c).

t.), 7.26 (2H, d). Elemental analysis: calc. for C₂₉H₁₇N₉O₂: C = 66.53, H = 3.27, N = 24.08. Found: C = 67.05, H = 3.47, N = 24.01%. ν_{max} (KBr)/cm⁻¹ 1584, 1541, 1463 and 1431. *m/z* (EI, low resolution) 523 (M⁺ requires 523.15), 445 (M⁺ – pyridyl. C₂₄H₁₃N₈O₂ requires 445.12) and others.

Fabrication and measurements of OLEDs

OLEDs fabricated in this work had a configuration of ITO/NPB (50 nm)/Alq (20 nm)/ET layer (30 nm)/Mg : Ag (10 : 1 by volume) alloy as shown in Fig. 2b (*x* = 30 nm). *N,N'*-Dinaphthalen-1-yl-*N,N'*-diphenyl-biphenyl-4,4'-diamine (NPB) and Alq were used as the HT layer and emissive layer, respectively. An indium-tin-oxide (ITO)-coated glass substrate with a sheet resistance of 14 Ω square⁻¹ treated by O₂-plasma for 5 minutes in advance was used as the substrate and anode. We also fabricated the ITO/NPB (50 nm)/Alq (40 nm)/Bpy-OXD (10 nm)/Mg : Ag device (see Fig. 2b, *x* = 10 nm) to investigate the ET property of Bpy-OXD and the ITO/NPB (50 nm)/Alq (50 nm)/Mg : Ag (see Fig. 2c) as a reference. All layers were sequentially deposited on the ITO-coated glass substrate at a pressure of 6 × 10⁻⁴ Pa or less. The emissive area of the device was 2 × 2 mm². The current density–applied voltage–luminance characteristics of OLEDs were measured using a Hewlett Packard HP4140B electrometer and a Topcon BM-7 luminance colorimeter. Durability measurements of OLEDs were performed at a constant current density of 25 mA cm⁻² with sealed devices, which were encapsulated under a dry N₂ gas (dew point of below –60 °C, O₂ concentration of below 10 ppm) with a fresh desiccant.

Results and discussion

Thermal and electronic properties

Fig. 3 shows DSC curves of the new bipyridyl-substituted oxadiazole derivatives (Bpy-OXD). An endothermic peak due to melting was observed at 267 °C in the first heating of Bpy-OXD as shown in Fig. 3a. A baseline shift due to the glass transition, an exothermic peak due to crystallization, another endothermic peak, and the endothermic peak of melting were observed in a second heating of Bpy-OXD. The endothermic peak at 250 °C should be caused by a crystal phase transition. On the other hand, an endothermic peak due to melting was recorded at 235 °C in the first heating of Bpy-OXDpy, as shown in Fig. 3b, and this was no longer detected in a second heating. A baseline shift due to the glass transition only appeared in a second heating. These DSC results confirmed that Bpy-OXD formed a stable glassy state with glass transition temperatures (T_g) of 106 °C and 114 °C for Bpy-OXD and Bpy-OXDpy, respectively. Since these T_g values were comparable to that (94 °C) of NPB, a practical HT material, the Bpy-OXD are practical thermally stable materials. XRD of Bpy-OXD thin films also confirmed the formation of a stable glassy state, showing only hollow curves in the XRD patterns.

UV-visible absorption and fluorescence spectra of neat thin films of Bpy-OXD are shown in Fig. 4. The absorption maxima of both materials were 280 nm and the materials emitted bright UV fluorescence. The band gaps of 3.64 eV for Bpy-OXD and 3.58 eV for Bpy-OXDpy, which were determined by the absorption edge of the UV and visible absorption spectrum of each neat thin film (see Fig. 4), were very wide. These wide band gap characteristics resulted from the weak π -conjugations of oxadiazole and, in addition, *meta* linkage in all phenyl and pyridyl rings. LUMO levels of the compounds (Bpy-OXD: 2.92 eV, Bpy-OXDpy: 2.67 eV) in a neat solid were low enough to easily accept electrons from a cathode metal such as Mg : Ag (work function: 3.7 eV). This nature was caused by molecular-level hybridization of two electrophilic moieties (pyridine and oxadiazole).¹⁸ In addition,

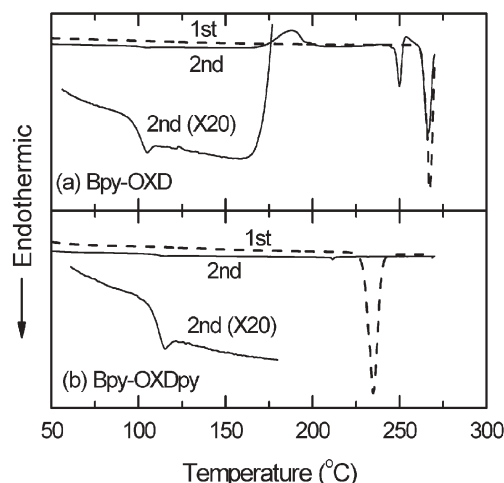


Fig. 3 DSC curves of (a) Bpy-OXD and (b) Bpy-OXDpy in the first (dashed line) and the second (solid line) heating.

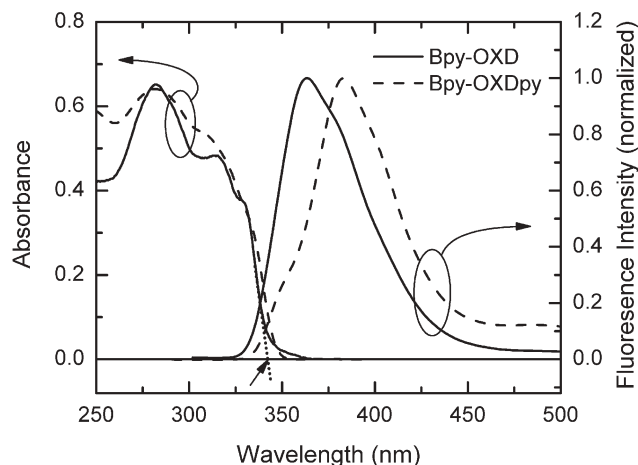


Fig. 4 UV and visible absorption and fluorescence spectra of 100 nm-thick vacuum deposited Bpy-OXD thin films. The black straight arrow indicates the absorption edge used to determine the band gap of Bpy-OXD.

HOMO levels of the materials (Bpy-OXD: 6.56 eV, Bpy-OXDpy: 6.25 eV) were sufficiently deep to suppress hole-leakage from the emissive layer to the cathode *via* the Bpy-OXD layer, and the hole confinement in the emissive layer yielded high quantum efficiencies of EL. In addition, the HOMO level of Bpy-OXD was 0.16 eV, smaller than that of a typically used HB material, bathocuproine (6.40 eV).¹⁹ Bpy-OXD can be utilized as efficient ET and HB materials with high thermal stability.

OLED performance

To evaluate the performance of Bpy-OXD as ET materials, we fabricated several OLEDs with Bpy-OXD as ET layers. Fig. 5 shows luminance *vs.* applied voltage and luminance *vs.* current density characteristics of the Bpy-OXD OLEDs, and Table 1 summarizes the performance of the OLEDs. As shown in Fig. 5a, the OLEDs with Bpy-OXD showed bright luminescence at a lower voltage than the reference device. Furthermore, the OLEDs with Bpy-OXD also exhibited higher current efficiency ($>6 \text{ cd A}^{-1}$) than the reference device, as shown in Fig. 5b and Table 1. These tendencies indicated the following: 1) an enhancement of the charge balance in the emissive layer based on efficient feeding of electrons into the emissive layer and 2) a reduction in hole-leakage caused by efficient hole confinement by the deep HOMO level of Bpy-OXD. In addition, as the thickness of the Bpy-OXD layer increased, the turn-on voltage became smaller. This result also suggested efficient ET in Bpy-OXD, because the HOMO level of Bpy-OXD was so deep that holes were sufficiently confined in the Alq emissive layer; that is, the recombination zone was restricted to the Alq layer, and therefore, the thicker Bpy-OXD device needed to transport electrons for a longer distance than the thin Bpy-OXD (10 nm) device. Also, it should be noted here that the reduction in turn-on voltage observed for the 10 nm-thick Bpy-OXD device strongly indicated the usefulness of Bpy-OXD as an electron injection material.

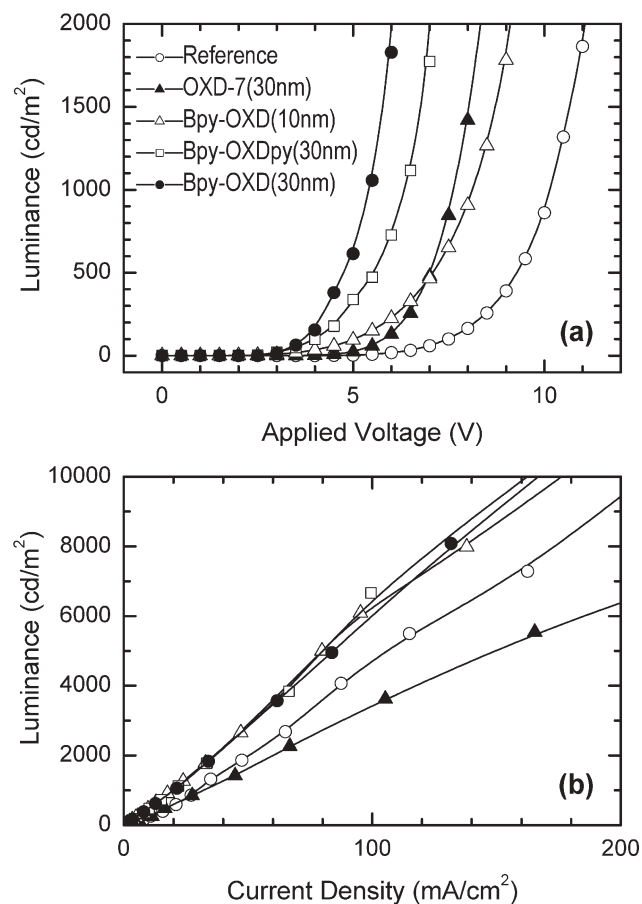


Fig. 5 Luminance vs. applied voltage (a) and luminance vs. current density (b) characteristics of OLEDs, whose structure is ITO/NPB(50 nm)/Alq(50 - x nm)/ET layer(x nm)/Mg : Ag(200 nm). Symbols indicate the material and thickness of the ET layer with the exception of the reference device.

Fig. 5 also shows the luminance vs. voltage and luminance vs. current density characteristics of a device with a 30 nm-thick Bpy-OXDpy layer. As indicated in the figures and Table 1, the device showed similar performance to the corresponding Bpy-OXD device. Therefore, the two bipyridyl substituted oxadiazole compounds are potentially useful as ET and HB materials and also as materials for the electron injection layer in OLEDs. However, the luminance vs. voltage characteristics of the Bpy-OXDpy device were slightly poorer than those of the Bpy-OXD device. A higher LUMO level of the Bpy-OXDpy (2.67 eV) than that of Bpy-OXD (2.92 eV)

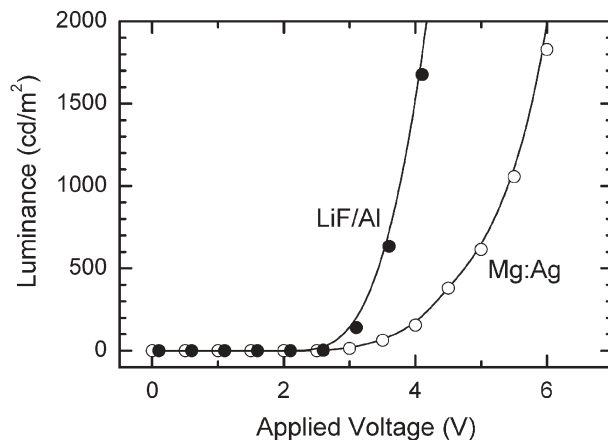


Fig. 6 Luminance vs. applied voltage characteristics of OLEDs of 30 nm-thick Bpy-OXD layer with different cathodes, whose structure is ITO/NPB(50 nm)/Alq(20 nm)/Bpy-OXD(30 nm)/cathode (Mg : Ag or LiF/Al). The LiF/Al cathode was composed of LiF(0.5 nm) and Al(200 nm).

caused the slightly lower performance. On the other hand, each Bpy-OXD device exhibited better performance than another reference device using OXD-7 (ref. 10), a representative oxadiazole ET derivative at the same thickness. The LUMO level of OXD-7 was also low (2.8 eV) enough to easily accept electrons from the cathode. Hence, the better performance of Bpy-OXD compared to OXD-7 is probably due to it containing no bulky substituents that lack electronic function, like *tert*-butyl.

Fig. 6 shows the luminance–voltage characteristics of a device with a 0.5 nm-thick LiF thin layer as an electron injection buffer and an Al cathode, where the structure of the organic multilayer is equal to that of the device with a 30 nm-thick Bpy-OXD layer using an Mg : Ag cathode. As shown in Fig. 6, the LiF/Al device showed higher luminance than the Mg : Ag cathode device; specifically, it attained a luminance of 500 cd m^{-2} at an applied voltage of only 3.4 V. Therefore, the LiF layer can work as an efficient electron injection buffer for Bpy-OXD as well as Alq and other conventional ET materials.²⁰ The current efficiency of the device, however, was lower than that of the corresponding Mg : Ag device, as shown in Table 1, and this confirmed the high ET efficiency in the Bpy-OXD layer; that is, overfeeding of electrons into the emissive layer was caused by combining an efficient ET material (Bpy-OXD) and effective electron injection buffer material (LiF). It should be noted that using

Table 1 Summarized performance of the OLEDs with Bpy-OXD as ET materials

Entry	V_{on}/V	$L_{\text{max}}^b/\text{cd m}^{-2}$	$\eta_c^c/\text{cd A}^{-1}$	$\eta_p^d/\text{lm W}^{-1}$ at luminance of 1000 cd m^{-2}
Bpy-OXD (10 nm)	3.1	24000 at 12.5 V	6.4	2.0 at 8 V
Bpy-OXD (30 nm)	2.9	25900 at 9 V	6.2	2.8 at 5.5 V
Bpy-OXDpy (30 nm)	2.7	26500 at 10 V	6.7	2.5 at 6.5 V
OXD-7 (30 nm)	4.6	16900 at 12 V	3.5	1.3 at 7.7 V
Reference	5.6	18300 at 15 V	4.8	1.0 at 10 V
Bpy-OXD (30 nm)/LiF/Al	2.6	38200 at 7.6 V	3.6	2.5 at 3.8 V

^a V_{on} is defined as the applied voltage for determining the luminance of 10 cd m^{-2} . ^b L_{max} is the maximum luminance, representing the applied voltage for determining the luminance. ^c η_c is the maximum current efficiency. ^d η_p indicates the power efficiency at the luminance of 1000 cd m^{-2} , representing the applied voltage for determining the efficiency.

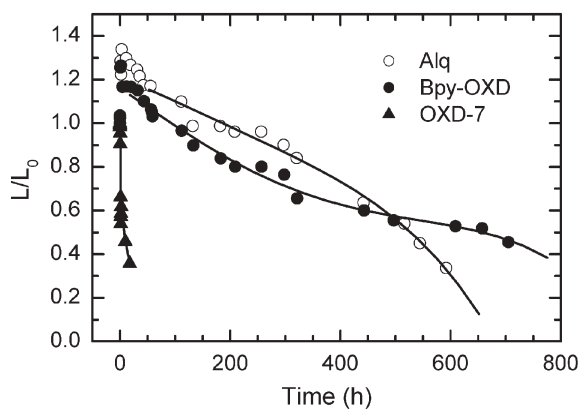


Fig. 7 Luminescence intensity changes (normalized by the initial luminance) of the Bpy-OXD device and reference devices with long-term continuous operation (constant current of 25 mA cm^{-2}). The solid lines are guides for the eye. Device structures are described in the main text.

efficient hole injection and modifying the transportation will probably lead to brighter and more efficient luminescence at a low operating voltage.

Finally, we tested the long-term operational durability of Bpy-OXD in OLEDs. Fig. 7 shows the luminance changes for continuous operation at 25 mA cm^{-2} of a Bpy-OXD device and reference devices using the practical ET material Alq and a representative oxadiazole ET material OXD-7. Their device structures were: ITO/CuPc(20 nm)/NPB(40 nm)/Alq(20 nm)/Bpy-OXD(30 nm)/LiF(0.5 nm)/Al(200 nm), ITO/CuPc/NPB/Alq(50 nm)/LiF/Al, and ITO/CuPc/NPB/Alq/OXD-7/LiF/Al. A CuPc (copper phthalocyanine) layer was inserted to give the device high durability, which is a well-known technique.⁵ Note that the test devices were encapsulated under dry N_2 gas with a fresh desiccant. As shown in Fig. 7, the Bpy-OXD device exhibited much better durability than the OXD-7 device and comparable durability to the reference device using the durable ET material Alq. Further detailed investigations are required, but these preliminary results nonetheless strongly suggest that the new bipyridyl-substituted oxadiazole compounds potentially have practical durability. We believe that the much higher operation durability of Bpy-OXDs result from their high thermal stability.

Conclusion

We have demonstrated new efficient electron-transporting and hole-blocking materials for OLEDs. The bipyridyl-substituted oxadiazole derivatives formed a stable glassy state with a T_g

greater than $100 \text{ }^\circ\text{C}$ and emitted bright UV fluorescence. The band gaps of the compounds were very wide ($>3.5 \text{ eV}$). Moreover, the bipyridyl-substituted oxadiazole derivatives had excellent ET, HB and electron-accepting abilities and also exhibited good thermal stability and operation durability. Bipyridyl-substituted oxadiazoles are a promising candidate for ET and HB materials for OLEDs.

Acknowledgements

The authors thank Dr Y. Nakajima and Mr D. Yamashita of Riken Keiki for measuring the ionization potential of compounds with their special photoelectron spectroscopic equipment (Riken Keiki AC-3). This work was supported by the Cooperative Link for Unique Science and Technology for Economy Revitalization (CLUSTER) of Japan's Ministry of Education, Culture, Sports, Science and Technology. It was also supported by the Ministry's 21st Century COE program and the Ministry's Grand-in-Aid (No. 16760009) to M.I.

References

- 1 C. W. Tang and S. A. VanSlyke, *Appl. Phys. Lett.*, 1987, **51**, 913.
- 2 C. Adachi, T. Tsutsui and S. Saito, *Appl. Phys. Lett.*, 1990, **57**, 531.
- 3 Y. Shirota, *J. Mater. Chem.*, 2000, **10**, 1.
- 4 U. Mitschke and P. Baeuerle, *J. Mater. Chem.*, 2000, **10**, 1471.
- 5 S. A. VanSlyke, C. H. Chen and C. W. Tang, *Appl. Phys. Lett.*, 1996, **69**, 2160.
- 6 M. Thelakkat and H.-W. Schmidt, *Adv. Mater.*, 1998, **10**, 219.
- 7 K. Katsuma and Y. Shirota, *Adv. Mater.*, 1998, **10**, 223.
- 8 H. Tanaka, S. Tokito, Y. Taga and A. Okada, *Chem. Commun.*, 1996, 2175.
- 9 C. Adachi, T. Tsutsui and S. Saito, *Appl. Phys. Lett.*, 1989, **55**, 1489.
- 10 Y. Hamada, C. Adachi, T. Tsutsui and S. Saito, *Jpn. J. Appl. Phys.*, 1992, **31**, 1812.
- 11 K. Tamao, M. Uchida, T. Izumizawa, K. Furukawa and S. Yamaguchi, *J. Am. Chem. Soc.*, 1996, **118**, 11974.
- 12 M. Uchida, T. Izumizawa, T. Nakano, S. Yamaguchi, K. Tamao and K. Furukawa, *Chem. Mater.*, 2001, **13**, 2680.
- 13 J. Bettenhausen and P. Stroehriegel, *Adv. Mater.*, 1996, **8**, 507.
- 14 S. B. Heidenhain, Y. Sakamoto, T. Suzuki, A. Miura, H. Fujikawa, T. Mor, S. Tokito and Y. Taga, *J. Am. Chem. Soc.*, 2000, **122**, 10240.
- 15 R. G. Kepler, P. M. Beeson, S. J. Jacobs, R. A. Anderson, M. B. Sinclair, V. S. Valencia and P. A. Cahill, *Appl. Phys. Lett.*, 1995, **66**, 3618.
- 16 P. Stroehriegel and J. V. Grazulevicius, *Adv. Mater.*, 2002, **14**, 1439.
- 17 R. Huisgen, J. Sauer, H. Stern and H. Markgraf, *Chem. Ber.*, 1960, **93**, 2106.
- 18 P. K. Ng, X. Gong, Suk Hang Chan, L. S. M. Lam and W. K. Chan, *Chem. Eur. J.*, 2001, **7**, 4358.
- 19 M. A. Baldo, C. Adachi and S. R. Forrest, *Phys. Rev. B*, 2000, **62**, 10967.
- 20 L. S. Hung, C. W. Tang and M. G. Mason, *Appl. Phys. Lett.*, 1997, **70**, 152.